A Compact E-Shaped Patterned Ground Structure and Its Applications to Tunable Bandstop Resonator

Shao Ying Huang, *Member, IEEE*, and Yee Hui Lee, *Member, IEEE*

***Abstract*—In this paper, an E-shaped patterned ground microstrip bandstop resonant cell is proposed. In comparison to other bandstop resonators, it provides the advantages of a high-Q factor, and a sharp transition knee within a small circuit area. This resonant cell is applied to the design of a tunable bandstop resonator. Due to the unique E-shaped pattern etched in the ground plane, the proposed resonant cell is able to provide tuning function within a small circuit area.**

***Index Terms*—Defected ground structure, patterned ground structures, slotted ground structures, tunable bandstop filters, tunable bandstop resonators.**

I. Introduction

MICROSTRIP lines with patterned ground plane such as slots or/and etched patches have attracted a lot of attention in the research society due to their unique characteristics including a prominent stopband and slow-wave effect [1]–[5]. They are also referred to as defected ground structure or slotted ground structure. These structures exhibit advantages such as ease of fabrication and compatibility with monolithic microwave integrated circuits. Various patterned ground structures have been proposed for filter designs [5] and for optimization of microwave devices, such as amplifiers [6].

Based on the characteristics of the stopband, these patterned ground structures can be categorized into electromagnetic bandgap (EBG) structures [1]–[4] and bandstop resonators [5], [7]–[13]. EBG structures provides a wide stopband with high attenuation. Therefore, they are often applied to the suppression of the unwanted frequencies over a wide frequency range [6]. However, they are restricted by the Bragg reflection condition, which requires a large circuit area for the EBG structure, especially for low working frequencies. On the other hand, bandstop resonators show flexibility. They can be cascaded [14] or superposed [15] to obtain a wide or an ultra-wide stopband. They have been successfully applied to low-pass filter designs to implement the series inductors, resulting in a sharp cutoff, wide bandwidth, and high attenuation of the stopband, and yet their size is still relatively small when compared to a conventional stepped-impedance low-pass filter [5], [9], [16]. Recently, they are applied to the design of tunable bandstop resonators [11], [12], which are used as harmonic traps integrated with tunable amplifiers or antennas to improve circuit performance.

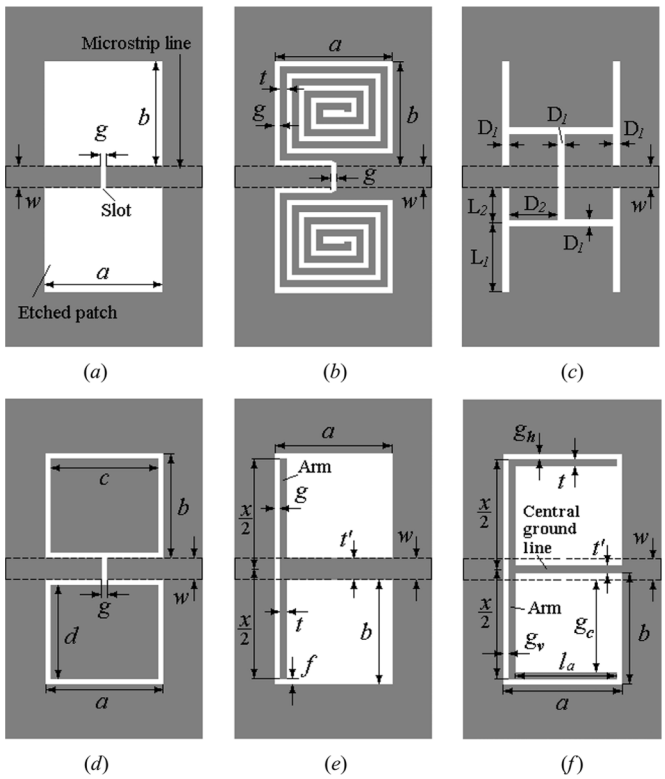

Fig. 1. Patterned ground microstrip bandstop resonator. (a) Dumbbell shaped [5]. (b) Spiral shaped [8]. (c) Double-H shaped [9]. (d) Modified dumbbell shaped [10]. (e) T shaped [12]. (f) E shaped.

Fig. 1(a)-(e) shows the schematics of the patterned ground structures that have been proposed in the literature. The dumbbell-shaped cell [5] in Fig. 1(a) is one of the first patterned ground structures. Based on this structure, many other modified and new patterned ground structures with improved performances were proposed [7]–[9]. The development of patterned ground structure is focused on the reduction in overall physical size of the structure, the improvement in the sharpness of the transition knee, and the increase in the Q factor. An unloaded Q factor is an important parameter that can be used to evaluate the intrinsic loss of a resonant circuit [17]. The shape of the etched patch in a dumbbell-shaped patterned ground structure could changed from square to arrow-shaped or circular [7]. The change in the shape of the etched patch has minor effect on the performance and physical size of dumbbell-shaped patterned ground structure. The performance is improved significantly in terms of the sharpness of the transition knee by the introduction of a spiral-shaped patterned ground structure [8]

Manuscript received May 16, 2008; revised September 20, 2008. First published February 13, 2009; current version published March 11, 2009.

The authors are with the School of Electrical and Electronic Engineering, Nanyang Technological University, Singapore 639798

Color versions of one or more of the figures in this paper are available online at http://ieeexplore.ieee.org.

Digital Object Identifier 10.1109/TMTT.2009.2013313

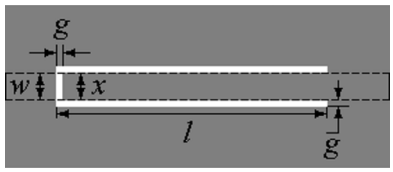

Fig. 2. U-slot patterned ground microstrip bandstop resonator [13].

shown in Fig. 1(b). In [9], a double-H-shaped resonant cell [see Fig. 1(c)] was proposed with both significant reduction in the physical size and enhancement of the sharpness of the transition knee as compared to a dumbbell-shaped cell [7]. In [10], the conventional dumbbell-shaped patterned ground structure is further modified by inserting a patch in the middle of each etched patch [see Fig. 1(d)]. The modified structure shows an increase in capacitance, resulting in a reduction in circuit area. Moreover, due to the modification, the tunability of the structure becomes possible by inserting varactors between the inserted patch and ground plane. A frequency tuning range of 19% is demonstrated in [11].

Recently, a T-shaped patterned ground structure [see Fig. 1(e)] is proposed to achieve a significant improvement in performance together with a large reduction in size [12]. In this structure, the slot of the dumbbell-shaped patterned ground structure in Fig. 1(a) is moved to the edges of the etched patch with arms and it is lengthened, forming a T-shape. Among the patterned ground structures compared in [12] that have a fixed resonant frequency, this structure has the smallest physical size and the sharpest transition knees. With the lengthened slot, it becomes possible to embed a varactor into the arms so as to allow for the tuning of the resonant frequency. A maximum frequency tuning range of 13.2% is realized.

Based on the T-shaped patterned ground structure in [12], we propose an E-shaped patterned ground structure [see Fig. 1(f)] to further improve the sharpness of the transition knee and to reduce the circuit area. In order to miniaturize the proposed E-shaped structure further, the design concept of a U-slot patterned ground structure [13] is adopted. Fig. 2 shows a U-slot patterned ground structure in [13]. As can be seen in Fig. 2, a U-slot cell consists of three connected slot lines in the ground plane below the microstrip line, forming a U-shaped slot. It is compact due to the unique U-slot configuration. For all six structures shown in Fig. 1, only the T-shaped and the proposed E-shaped structure can adopt a geometry similar to the U-slot structure.

In this paper, an E-shaped patterned ground structure that adopts the geometry of the U-slot structure is proposed. This structure outperforms all the patterned ground structure reviewed in the literature in terms of physical size, sharpness of the transition knee, and unloaded Q factor. Furthermore, the proposed structure is applied to realize a compact tunable bandstop resonator. The proposed structure is designed in Section II. Also in Section II, this structure is compared to other patterned ground structures in the literature in terms of physical size, frequency response (sharpness of the transition knees, attenuation at the resonant frequency, insertion loss in the passbands), and the Q factor. An equivalent circuit model is also proposed in Section II. In Section III, the effect of the variation of different dimensions of the proposed structure on its performance are studied. The design and modeling of a tubable bandstop resonator by employing the proposed E-shaped structure is presented in Section IV.

II. Design of the E-Shaped Patterned Ground Microstrip Resonator

A. Physical Size and Resonant Frequency of Patterned Ground Structures

In a dumbbell-shaped bandstop resonator, the size of the two etched rectangular patches has to be increased in order to obtain a decrease in the resonant frequency. However, this results in an overall increase in the circuit area of the cell. It has always been a challenge for a patterned ground structure to obtain a low resonant frequency and a small circuit area simultaneously. In order to obtain a compact resonator at a low frequency, a spiral-shaped etched pattern [see Fig. 1(b)] is introduced in the etched patch of the dumbbell [8]. With the spiral-shaped etched pattern, the size of the cell can effectively be reduced with a fixed resonant frequency. Similarly, a double-H-shaped resonator [9] [see Fig. 1(c)] or a modified dumbbell-shaped structure (with an inserted patch in the middle of each etched patch) [10] [see Fig. 1(d)] can provide a reduction in circuit area of the cell at a fixed resonant frequency. Keeping the resonant frequency constant, the cell size can further be decreased by using a T-shaped etched pattern with a lengthened slot [12] [see Fig. 1(e)]. The report on a U-slot structure [13] presents a big progress in the development of patterned ground structures in terms of circuit miniaturization. Rectangular etched patches are not required in a U-slot structure, and thus it is more compact than the other dumbbell-shaped structures. A U-slot structure has two slot lines in the direction of the transmission line [see Fig. 2], keeping the structure compact. Of the five structures discussed, only the T-shaped structure can be tailored to be of similar dimension to the U-slot structure, as shown in Fig. 3(a). Moreover, a T-shaped structure is more compact than a U-slot structure when they are designed to resonate at the same frequency [12].

B. Proposed E-Shaped Patterned Ground Structure

The E-shaped patterned ground microstrip resonator proposed in this paper is shown in Fig. 1(f). As shown, the lengthened slot in a T-shaped structure is further extended to the two edges of the etched patches that are in parallel to the microstrip line, forming the E-shaped structure. The dimensions of this E-shaped structure are as labeled in Fig. 1(f). The width of the the metal strip below the microstrip line (central ground line), t', is reduced to enhance the inductive effect. Similar to the T-shaped structure, the proposed E-shaped structure can further be miniaturized by adopting a U-slot geometry, as shown in Fig. 3(b). In Fig. 3(b), x of the E-shaped structure is set to be as large as the width of the microstrip line, w, and t' is tailored.

Seven resonant cells from Figs. 1(a)–(d), 2, and 3(a) and (b) are designed to resonate at 5 GHz. Taconic ($\epsilon_r = 2.45, h = 0.4$ mm) is used as the substrate. The dimensions of the structures are tabulated in Table I. For structures in Fig. 1(a)–(d),

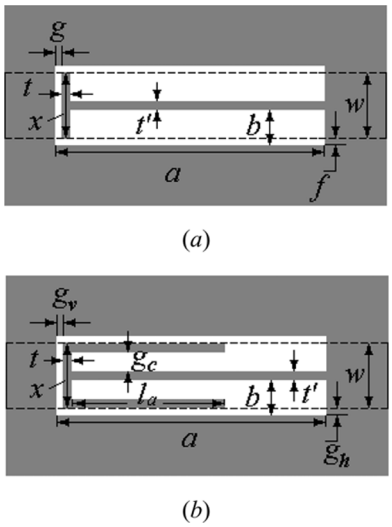

Fig. 3. Slotted ground microstrip bandstop resonator adopted U-slot geometry. (a) T-shaped structure [12]. (b) New proposed E-shaped structure.

TABLE I
DIMENSIONS OF PATTERNED GROUND MICROSTRIP BANDSTOP RESONATORS IN FIGS. 1 AND 2 RESONATING AT 5 GHz (UNIT: MILLIMETERS)

Figure	Dimensions
Fig. 1 (a)	$w = 1.14$, $a = b = 10.00$, $g = 0.25$
Fig. 1 (b)	$w = 1.14$, $a = b = 2.90$, $g = 0.25$, $t = 0.30$
Fig. 1 (c)	$w = 1.14$, $D_1 = 0.50$, $D_2 = 2.65$, $L_1 = 4.08$, $L_2 = 2.72$
Fig. 1 (d)	$w = 1.14$, $a = b = 8.20$, $g = 0.25$, $c = d = 7.70$
Fig. 2	$w = x = 1.40$, $l = 11.30$, $g = 0.25$
Fig. 3 (a)	$w = x = 1.40$, $a = 11.00$, $b = 0.80$, $g = f = 0.25$, $t = t' = 0.30$
Fig. 3 (b)	$w = x = 1.40$, $a = 5.20$, $b = 0.80$ $g_h = g_v = 0.25$, $t = t' = 0.30$, $l_a = 4.70$

$w = 1.14$ mm corresponding to a characteristic impedance of 50 Ω. For those in Figs. 2 and 3(a) and (b), the width of the microstrip line is set to be 1.40 mm in order to accommodate the arms of the proposed E-shaped structure. It is tapered to 1.14 mm at two ends for a load matching. x in the U-slot, T-shaped, and E-shaped structure is set to be 1.40 mm, $x = w$. All these structures are simulated using a full-wave EM simulator, Agilent Technologies' Advanced Design System (ADS). They are compared in terms of physical size, frequency response, and Q factor.

C. Physical Size

Fig. 4(a) and (b) shows the S_{21}-parameters of these resonant cells designed to resonate at 5 GHz. As can be seen in Fig. 4, all the structures resonate at 5 GHz according to the design specifications. Table II tabulates the overall length, width, and the area of these patterned ground structures in column two to four, respectively. The fifth column shows the area of the proposed E-shaped cell over that of the other resonant cells in percentage. The last column of Table II lists the calculated unloaded Q factors of the structures, which will be discussed shortly. As shown in Table II, with the same resonant frequency, the proposed E-shaped cell has the smallest circuit area. It is only 4.68% of the dumbbell-shaped structure and less than half of the size of the most recently proposed T-shaped structure (47.37%). This observation implies that the proposed E-shaped structure has the smallest physical size in all the resonant structures under this comparison when they are designed to resonate at 5 GHz.

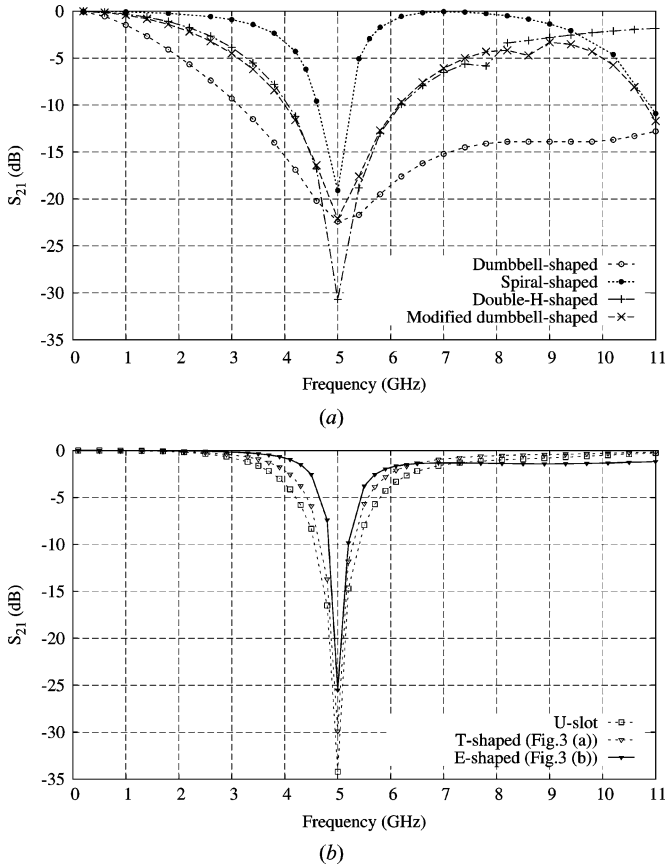

Fig. 4. S_{21}-parameters of the patterned ground structures when they are designed to resonate at $f_0 = 5$ GHz.

TABLE II
PHYSICAL SIZE OF PATTERNED GROUND MICROSTRIP BANDSTOP RESONATORS AT $f_0 = 5$ GHz

Resonator Cell	Width (mm)	Length (mm)	Area (mm^2)	E-shaped /other cell (%)	*Q-factor*
Dumbbell	21.1	10.0	211.4	4.68	4.3
Spiral-shaped	6.9	2.9	20.1	49.7	144.1
Double-H	14.7	6.8	100.2	9.88	28.0
M. Dumbbell	17.5	8.2	143.9	6.88	8.3
U-slot	1.9	11.3	21.5	46.05	557.6
T-shaped	1.9	11	20.9	47.37	639.4
E-shaped	1.9	5.2	9.9	100	714.6

D. Frequency Response

The frequency responses of the patterned ground structures resonating at 5 GHz are compared in terms of sharpness of the transition knee, attenuation at the resonant frequency, and insertion loss within the passband. In general, a bandstop resonator is used for harmonic suppression. When it comes to harmonic suppression, a sharp transition knee, high resonant attenuation, and small insertion loss in both lower and higher passband is

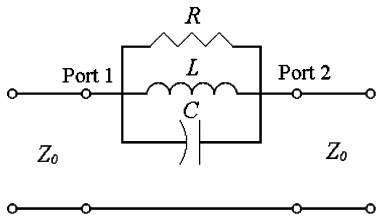

Fig. 5. Equivalent circuit model for the E-shaped bandstop resonator.

desirable. When a bandstop resonator is applied to suppress harmonics, the sharper the transition knee of the resonator the less insertion loss it introduces to the desired frequencies. High attenuation is to provide effective suppression of unwanted frequencies and small insertion loss within the passbands is to minimize the loss of the wanted frequencies.

In Fig. 4(a) and (b), it can be seen that the resonant cells with the same resonant frequency exhibit different sharpness of the transition knee. Comparing Fig. 4(a) and (b), among all the structures, the conventional dumbbell-shaped cell has the flattest transition knee. The proposed E-shaped cell has a sharpest lower transition knee and a similar upper transition knee to the spiral-shaped cell. The E-shaped cell has the best performance in terms of transition knee. In terms of attenuation at the resonant frequency, the U-slot cell has the highest attenuation of -34 dB followed by the double-H-shaped cell with an attenuation of -31 dB and the T-shaped cell with an attenuation of -30 dB. The proposed E-shaped structure exhibits an attenuation of -26 dB, which is the fourth highest attenuation in all the structures. Insertion loss in the lower passband is dependent on the lower transition knees, whereas that in the upper passband is affected by the upper transition knee and the second resonant frequency (how close it is to the first resonance) of the structure. As shown in Fig. 4, the dumbbell-shaped cell shows an insertion loss higher than -10 dB in the upper passband. The spiral-shaped and modified dumbbell-shaped cell exhibits the second resonance that is close to 11 GHz. The U-slot, double-H-shaped, and T-shaped cell have a decreasing insertion loss in the upper passband, while the proposed E-shaped structure shows a constant insertion loss at around -1.3 dB. Comparing the frequency response of the proposed E-shaped structure to other patterned ground structures, the E-shaped structure shows the best transition knee performance within the smallest circuit area.

E. Q Factor and Explanations

The unloaded Q factors of the patterned ground structures resonating at 5 GHz are calculated based on simulation results and compared. The circuit in Fig. 5 is proposed to model the E-shaped structure within the frequency range of interest (up to 11 GHz in this study). The R, L, and C value in the circuit are extracted using the following equations [18]:

$$C = \frac{w_c}{Z_0 g_1 \left(w_0^2 - w_c^2\right)} \tag{1}$$

$$L = \frac{1}{w_0^2 C} \tag{2}$$

$$R = \frac{2Z_0}{\sqrt{\dfrac{1}{|S_{11}(w_0)|^2} - \left(2Z_0\left(w_0 C - \dfrac{1}{w_0 L}\right)\right)^2 - 1}} \tag{3}$$

where w_c and w_0 are the cutoff and center angular frequency, respectively. Z_0 is the characteristic impedance of the transmission line. g_1 is the normalized element value in the Butterworth-type one-pole prototype low-pass filter circuit $g_1 = 2$ [5]. $S_{11}(w_0)$ is the reflection coefficient at the resonant frequency. Based on simulation results at $f_0 = 5$ GHz, the value of f_c and $S_{11}(w_0)$ of the E-shaped structure are extracted to be $f_c = 4.55$ GHz and $S_{11}(w_0) = 0.99$. The Q factor without external circuit for the parallel RLC resonant circuit is estimated using (4) as follows in [17]:

$$Q = \frac{\omega_0 w_T}{P} = \frac{\omega_0 2\langle w_e\rangle}{P} = \frac{\omega_0 2 \cdot \dfrac{1}{4} C|V|^2}{\dfrac{1}{2}\dfrac{1}{R}|V|^2} \tag{4}$$

where w_T is the total electromagnetic energy, P is the power loss, $\langle w_e\rangle$ is the time-averaged electric energy, and V is the voltage connecting the two ports of the circuit. By using (1)–(4), Q factor for the E-shaped structure is calculated to be 714.6. Note that R in (3) and (4) accounts for the loss of the resonator including loss through heat and radiation.

Q factors of other patterned structures in Fig. 1 are also estimated based on their simulated S-parameters [5], [8]–[10], [12], [13]. Their Q factors are tabulated in the last column of Table II. In Table II, the conventional dumbbell-shaped structure has the lowest Q factor at 4.3, indicating the highest loss. The Q factor of the modified dumbbell-shaped structure is close to that of dumbbell-shaped structure at 8.3. The Q factor of the double-H-shaped structure is almost seven times as much as that of the dumbbell cell (28.0). The spiral-shaped structure has a Q factor as high as 144.1.

The three cells with a U-slot geometry (including the U-slot cell itself) shows a significant increase in Q factor. This can be attributed to the strong field strength around the slot below the microstrip line when the transversal dimension (x in Figs. 2 and 3) of the etched patch is reduced. Among these three cells with high Q factor, the proposed E-shaped cell has the highest Q factor at 714.6. It is the highest Q factor among all the structures under comparison.

The three cells with a U-slot geometry are simulated using CST Microwave Studio. Fig. 6 shows the surface current of their ground planes at the resonant frequency. The size and color (in online version) of the arrows are proportional to the magnitude of the surface current. As can be seen in Fig. 6, currents are flowing around the etched patterns resulting in a periodic charging and discharging process. This charging and discharging process generates capacitive and inductive effect. Fig. 6(a) shows a sketch of the associated inductance and capacitance. With the above charging and discharging mechanism, the capacitance is determined by the current density and the width of the slot, whereas the inductance is determined by the length of the current path. Table III shows the extracted R, L, and C values from the equivalent circuit model in Fig. 5. The U-slot cell has the highest inductance due to the long current path [the

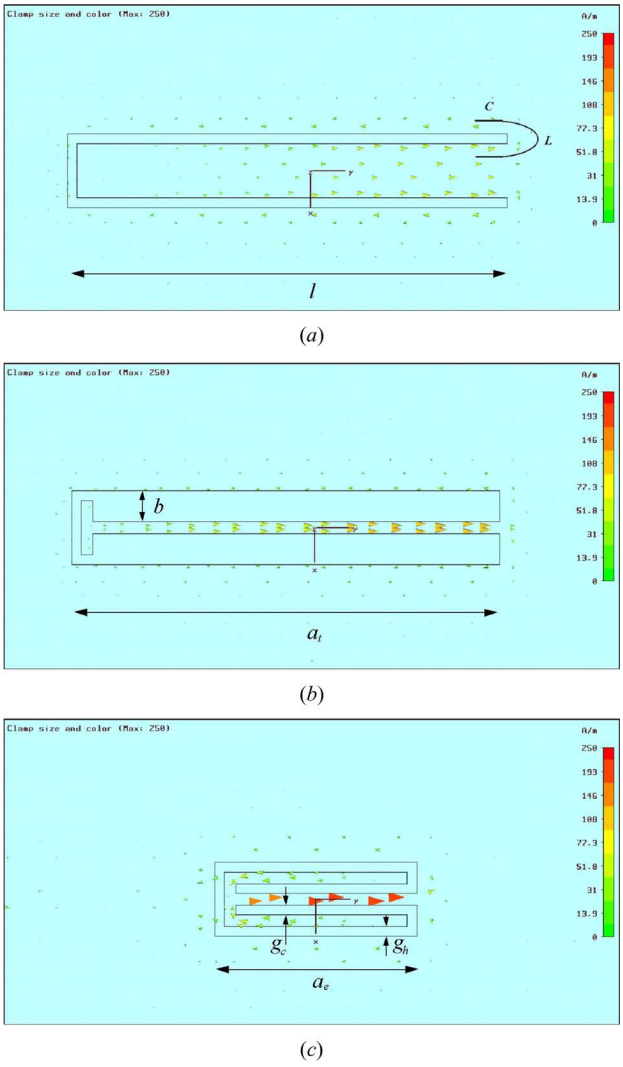

Fig. 6. Simulated surface current of the ground planes of the patterned ground structures. (a) U-slot patterned structure. (b) T-shaped structure. (c) E-shaped structure.

TABLE III
R, L, C OF THE CIRCUIT MODELS IN FIG. 5 FOR THE PATTERNED GROUND MICROSTRIP RESONATORS AT $f_0 = 5$ GHz

Resonator Cell	R ($k\Omega$)	L (nH)	C (pF)
U-slot	27.97	1.60	0.64
T-shaped	22.81	1.14	0.89
E-shaped	13.52	0.60	1.68

largest longitudinal dimension l in Fig. 6(a)]. For the T-shaped structure, the inductance is still high due to the long current path. Its capacitance is increased from the U-slot cell since the surface current density in the central line of the T-shape structure is increased. However, due to the large width of gaps in the longitudinal direction [b in Fig. 6(b)], the capacitance is increased only by a small amount. The E-shaped structure has the highest capacitance because it has two parts of equivalent capacitance: one between the central line and the extended arms (g_c in Fig. 6(c) where $g_c = b - g_h - t$) and the other is between the arms and

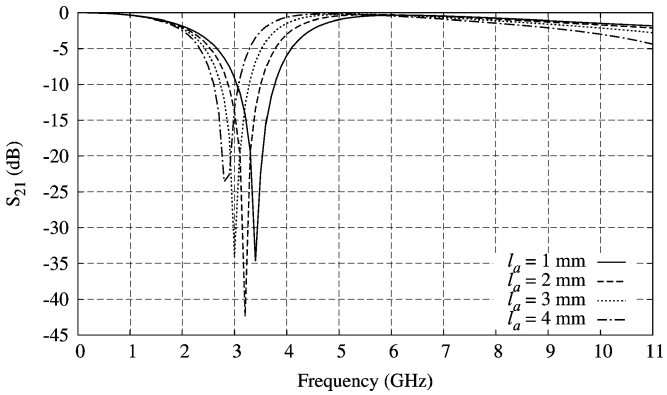

Fig. 7. S_{21}-parameters of the E-shaped bandstop resonators with different l_a ($w = 1.14$ mm, $a = b = 5$ mm, $g_h = g_v = 0.25$ mm, $t = t' = 0.3$ mm).

the edge of the etched patch [g_h in Fig. 6(c)]. Since there is high surface current density along the arm of the E-shaped structure, as shown in Fig. 6(c), the resultant capacitance is high. The inductance, on the other hand, is reduced due to the reduction in longitudinal path length ($a_e < a_t$ or l in Fig. 6). The high capacitance contributes to the significant increase in the Q factor of the proposed E-shaped structure with a simple modification to the patterned ground structure.

III. EFFECT OF THE DIMENSIONS

For the proposed E-shaped bandstop resonant cell, the effect of the dimensions, the horizontal arm length (l_a), the width of the central ground line (t'), and the gap width (g_h and g_v) on the performance of the resonator are studied based on simulation results. The structure in Fig. 3(b) with $a = b = 5$ mm is used in the study. Fig. 7 shows the transmission coefficients of the E-shaped structures when l_a is varied while the rest of the dimensions of the structure is kept constant. As can be seen in Fig. 7, when l_a increases, the resonant frequency f_0 decreases while the cutoff frequency f_c remains the same. Moreover, insertion loss in the upper passband increases as l_a increases. A negligible change in f_c indicates that l_a has insignificant contribution to the inductance L in the equivalent circuit. This is because that the surface current density at the end of the E-shaped arms is almost negligible, and thus, the change in the length of the current path of the arms of the patterned ground structure is neglected. Since the equivalent L is a constant, the shifting of f_0 to a lower frequency as l_a increases is because of a change in capacitance C. An increase in l_a causes an increase in the length of the gaps between the arms and the edge of the etched patch [g_h in Fig. 3(b)]. The capacitive effect between the central line and the extended arms [g_c in Fig. 3(b)] is negligible due to a large g_c in this part of study ($g_c = 4.45$ mm, $g_h = 0.25$ mm, $g_c \gg g_h$). Although the current density is not high at the end of the arms, the increase in l_a results in a notable increase in C due to the small width of the gaps. For the higher loss in the upper passband with a longer l_a, it is because the increase in l_a results in a shifting of the second resonance to lower frequencies.

Fig. 8 shows the simulated S_{21}-parameters of the proposed structures with a varied width of the central ground line t'. When $t' = 1.14$ mm, the width of the central ground line is equal to the width of the microstrip line above it. As seen in Fig. 8,

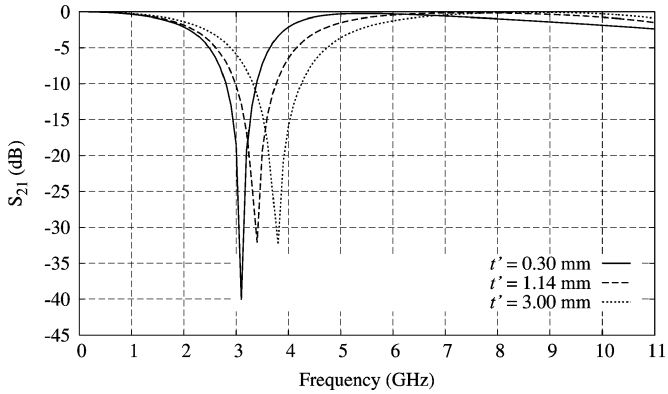

Fig. 8. S_{21}-parameters of the E-shaped bandstop resonators with different t' ($l_a = 2.20$ mm, $w = 1.14$ mm, $a = b = 5.00$ mm, $g_h = g_v = 0.25$ mm, $t = 0.30$ mm).

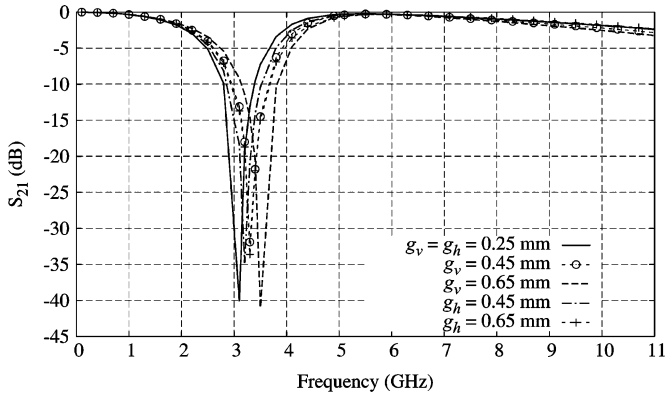

Fig. 9. S_{21}-parameters of the E-shaped bandstop resonators with different g_v or g_h ($l_a = 2.20$ mm, $w = 1.14$ mm, $a = b = 5.00$ mm, $t = t' = 0.3$ mm).

an increase in t' leads to an increase in both f_0 and f_c. This is because an increase in t' shortens the current path, thus reducing the equivalent inductance. The change in capacitance at g_c due to the increase in t' is neglected because g_c is large, as previously stated.

Fig. 9 shows the S_{21}-parameters of the E-shaped structures when g_v or g_h is varied. In Fig. 9, it is observed that f_c does not change with the width of the gap while f_0 increases when g_v or g_h increases. This is because that the width of the gap (vertical or horizontal) affects the equivalent C, but not L. L is not changed since the size of the etched patch remains the same (the length of the current path remains the same). It is also noticed that an increase in g_v introduces a larger increase in f_0 than the same amount of increase in g_h. This implies that g_v has more significant effect than g_h, which is due to the high surface current density around the microstrip line.

IV. E-Shaped Tunable Bandstop Resonator

A. Design and Circuit Model

The E-shaped tunable bandstop resonator is designed and implemented. In [12], a tunable bandstop resonator is implemented applying T-shaped patterned ground structure [see Fig. 1(e)] with varactors embedded in the arms. However, in a T-shaped structure, the length of the arms x has to be sufficiently large

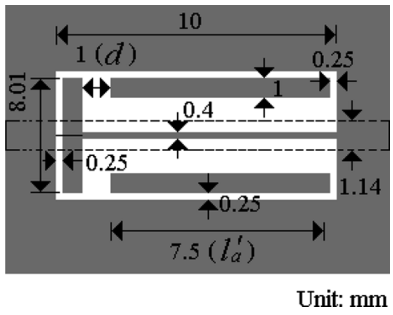

Fig. 10. Schematic of an E-shaped structure for realizing the tuning functionality.

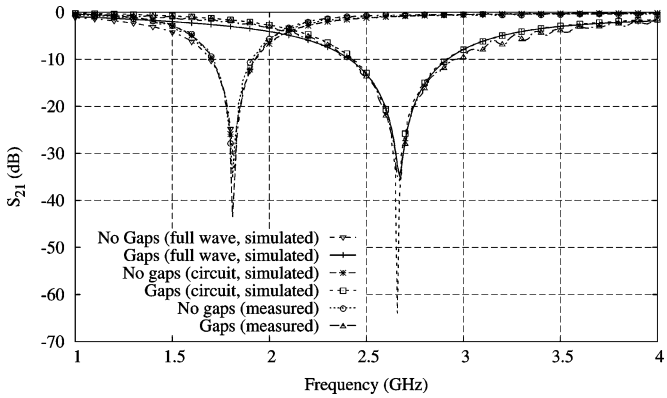

Fig. 11. S_{21}-parameters of the E-shaped structures with or without gaps in Figs. 3(b) and 10.

in order to accommodate the varactors, which results in a large circuit area of the structure. If the U-slot geometry is adopted to the T-shaped structure, as shown in Fig. 3(a), it becomes difficult to accommodate varactors.

In this proposed E-shaped bandstop resonator shown in Fig. 3(b), the extension arms make it possible for lumped circuit components to be embedded easily into the structure. Fig. 10 shows an E-shaped structure with two identical gap of length d. The gaps can be moved along the arms. The arms of length l'_a are coupled to the central ground line through the gaps. The strength of coupling is determined by d, the length of the gap in the arms.

Fig. 10 shows the E-shaped resonator with gap. It is used to demonstrate the tuning functionality of the proposed structure. Taconic ($\epsilon_r = 2.45, h = 0.4$ mm) is used as the substrate. The dimensions are labeled as shown in Fig. 10. $w = 1.14$ mm corresponding to a characteristic impedance of 50 Ω. In order to facilitate the fabrication and testing, $g_h = g_v = 0.25$ mm, $t = 1.00$ mm, and $t' = 0.40$ mm. The length of the arm, x is set to 8.01 mm in order to minimize interference caused by the embedded circuit components. This E-shaped structures without gap and with gap are simulated. Fig. 11 shows their simulated S_{21}-parameters. As shown in Fig. 11, the structure without gap shows a resonant frequency of 1.80 GHz, whereas the structure with gap shows a resonant frequency of 2.66 GHz.

Based on the equivalent circuit of an E-shaped structure in Fig. 5, a circuit model is proposed for the E-shaped structure with gaps [see Fig. 10] and shown in Fig. 12(a). As shown

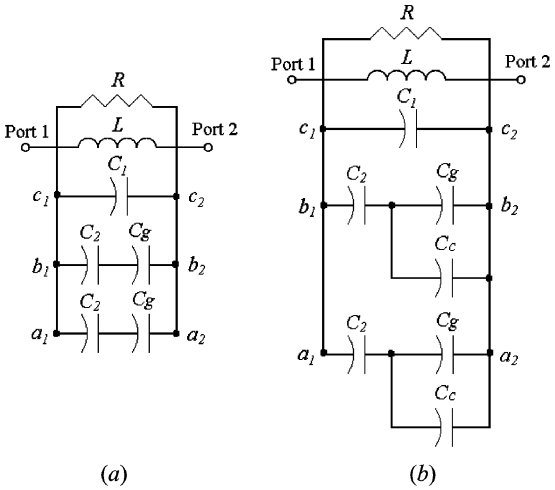

Fig. 12. Proposed circuit model for E-shaped structure: (a) with gaps and (b) with mounted capacitors across the gaps.

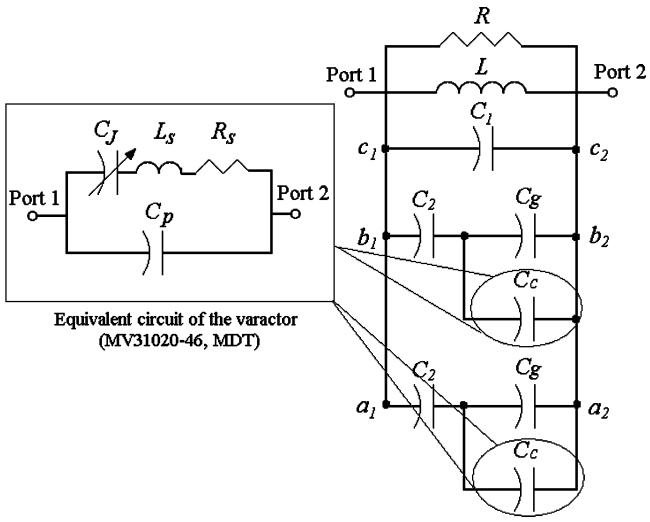

Fig. 13. Equivalent circuit of the tunable E-shaped bandstop resonator with varactors.

in Fig. 12(a), C_1 corresponds to coupling between the central ground line and the edge of the etched patches, while C_2 corresponds to that part of coupling between the arm with a length of l'_a and the edge of the etched patch. Therefore,

$$C_1 + 2C_2 \approx C \tag{5}$$

where C is the capacitance in the equivalent circuit of the E-shaped structure without gaps in Fig. 5. C_g is the new coupling between the arm l'_a and the central ground line introduced by the gap. Nodes of the circuit are labeled as shown in Fig. 12(a) for further analysis.

With C_g, the total capacitance between node $a_1a_2, C_{a_{12}}$ can be estimated using (6) as follows:

$$C_{a_{12}} = (C_2C_g)/(C_2 + C_g). \tag{6}$$

Based on (6), $C_{a_{12}} = C_2$ when there is no gap and C_g goes to infinity, resulting in $C_1+2C_{a_{12}} \approx C$ according to (5); $C_{a_{12}} < C_2$ when gaps are introduced and C_g is a finite number, leading to $C_1 + 2C_{a_{12}} < C_1 + 2C_2$; $C_{a_{12}} = 0$ and node a_1 and a_2 are disconnected when C_g is approaching 0. Based on the simulation results and (1)–(3), RLC in the equivalent circuit for the E-shaped structure without gap is obtained to be 289479.70 Ω, 3.25 nH, and 2.37 pF, respectively. Using a schematic, Agilent Technologies' Advanced Design System, C_g can be obtained by following the guidelines as follows: $C_1 + 2C_2 < C$ since a small portion of coupling between the arms to the edge of the etched patch is eliminated due to the gap; $C_1 > 2C_2$ due to the high confinement of electromagnetic fields around the microstrip line. With $C_1 = 1.1$ pF and $C_2 = 0.59$ pF, C_g is extracted to be 10^{-5} pF for the structures with gap ($C_g \approx 0$ and node a_1 and a_2 are equivalent to open circuit). The equivalent circuits for the E-shaped structure without gap and with gap are simulated. Fig. 11 shows their simulated S_{21}-parameters. As can be seen in Fig. 11, the simulation results of the equivalent circuits are in good agreement with those using a full-wave simulation.

In the design of an E-shaped patterned ground structure, when C_g is approaching 0 as that in the case above, C_1 can be estimated using (7) as follows:

$$C_1 = 1/\left(w_{0g}^2 L\right) \tag{7}$$

where w_{0g} is the angular resonant frequency of the E-shaped structure with gap.

The gaps along the arms allow accommodation of circuit components. If a capacitor is mounted across the gap, the circuit in Fig. 12(a) is modified to the circuit in Fig. 12(b) where the mounted capacitor introduces a C_c that is in parallel with C_g. With the mounted capacitors across the gaps, the total capacitance between node a_1a_2 changes and is denoted as $C'_{a_{12}}$. $C'_{a_{12}}$ can be expressed as follows when L_c is neglected in the derivation:

$$C'_{a_{12}} = (C_2(C_g + C_c)/(C_2 + C_g + C_c). \tag{8}$$

When $C_g \approx 0, C'_{a_{12}} \approx C_2C_c/(C_2 + C_c)$. According to (8), $C_2 > C'_{a_{12}} > C_{a_{12}}$, thus, $C > C_1+2C'_{a_{12}} > C_1+2C_{a_{12}}$ based on (5). Therefore, mounting capacitors across gaps tunes the resonant frequency within a range of frequencies between the frequency for the structure without gap and the frequency for the structure with gap. The structure becomes a tunable bandstop resonator when tunable capacitors or varactors are used. When varactors are embedded into the structure, the tuning range of the E-shaped resonator can be obtained based on the equivalent circuit in Fig. 12(b) and the specifications of the varactor.

The MV31020-46 varactors from the MDT Corporation, Westford, MA, are used in order to realize a tunable bandstop resonator. The equivalent circuit of the E-shaped structure with varactors is shown on the right of Fig. 13. The capacitor C_c in the equivalent circuit for the E-shaped structure with gap in Fig. 12(b) is replaced by the equivalent circuit of the varactor, as shown on the left of Fig. 13. C_J is the junction capacitance that can be estimated using (9) as follows [19]:

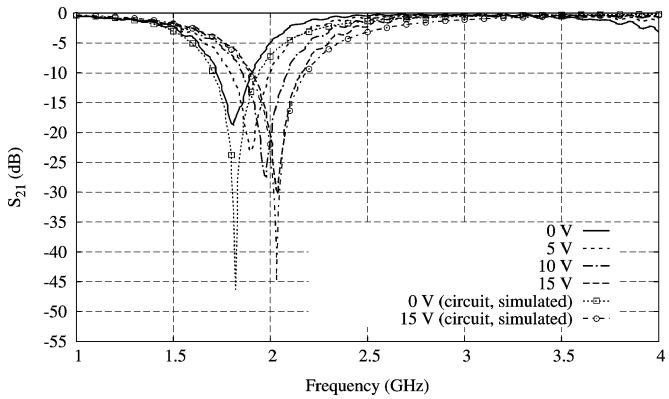

Fig. 14. Measured and simulated S_{21}-parameters of the tunable E-shaped bandstop resonator when varactors are mounted across the gaps.

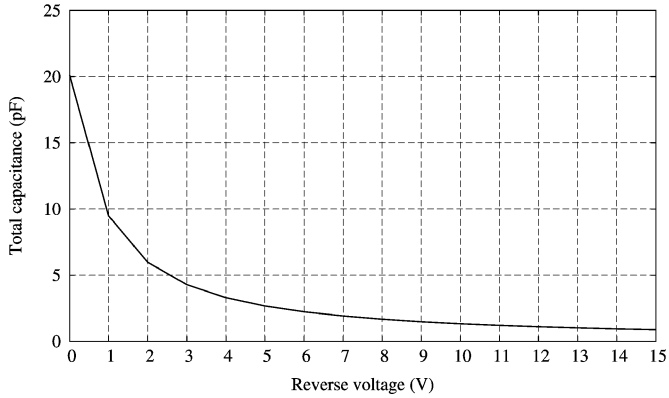

Fig. 15. *C–V* characteristics of the varactor used in the proposed tunable bandstop resonator.

$$C_J = \frac{C_{0j}}{\left(1 + \frac{V}{\Phi}\right)^{\gamma}} \text{ pF} \tag{9}$$

where C_{0j} is the junction capacitance at 0 V in picofarads, Φ is the built-in potential, V is the applied reverse voltage, and γ is the tuning slope. L_s is the parasitic inductance, R_s is the parasitic resistance, and C_p is the package capacitance. Fig. 14 shows the simulation results of this equivalent circuit when the dc bias is set to 0 and 15 V with $L_s = 0.170$ nH, $R_s = 0.497\ \Omega, C_p = 0.100$ pF, $C_{0j} = 20.007$ pF, $\Phi = 1.2$ V for GaAs, and $\gamma = 1.250$ [19]. As shown in Fig. 14, the equivalent circuit has a resonant frequency at 1.81 and 2.07 GHz when V is set to 0 and 15 V, respectively. The predicted tuning range is 12.4%.

B. Experiment

The E-shaped structure is fabricated. The measured S_{21}-parameters of the structure without a gap and with a gap are shown in Fig. 11 with their simulated results. As can be seen in Fig. 11, the E-shaped structure shows a resonant frequency 1.80 GHz when there is no gap in the structure, whereas a resonant frequency of 2.66 GHz when there is a gap. The measurement results agree well with the simulation results.

The MV31020-46 varactors are mounted across the gaps. Fig. 15 shows the capacitance–voltage (*C–V*) characteristics of this varactor. The tuning range for the capacitance is from 20 to 0.5 pF when the applied bias dc voltage is varied from 0 to 15 V.

Fig. 16(a) and (b) shows the photographs and schematic of the microstrip line of the implemented tunable bandstop resonator, respectively. Fig. 17 shows the photograph of its ground plane. DC voltage is supplied from the plane with a microstrip line, through a via, to the varactors on the other side of the board (the ground plane). On the plane with a microstrip line, an RF choke (47 nH with a self-resonant frequency at 2.6 GHz) is placed between the dc supply and the varactor in order to minimize RF loss of the circuit in the frequency range of interest. Moreover, the dc supply and RF chokes are located outside the the circuit area of the resonator so as to eliminate their possible effect on

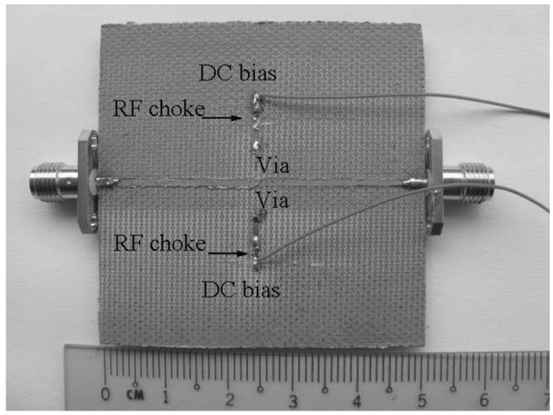

(*a*)

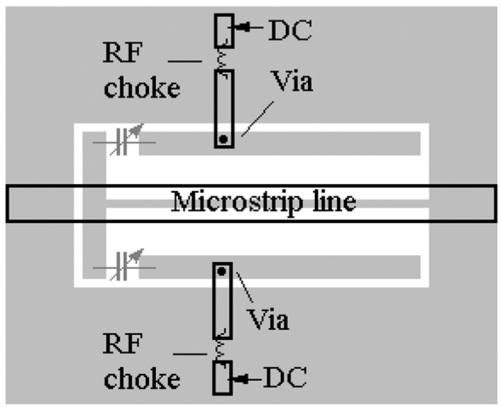

(*b*)

Fig. 16. Fabricated tunable E-shaped bandstop resonator with varactors and dc supply. (a) Photograph of the microstrip line side. (b) Schematic of the microstrip line side.

the resonant cell. In Fig. 16(b), the E-shaped pattern is etched in the ground plane. Vias are introduced to the arms and varactors are connected across the gaps.

Fig. 14 shows the measured S_{21}-parameters when varactors across the gaps have dc bias. As shown in Fig. 14, the E-shaped structure has a resonant at 1.81, 1.90, 1.97, and 2.07 GHz when dc bias of 0, 5, 10, and 15 V are supplied, respectively. This proposed E-shaped tunable bandstop resonator realize a tuning

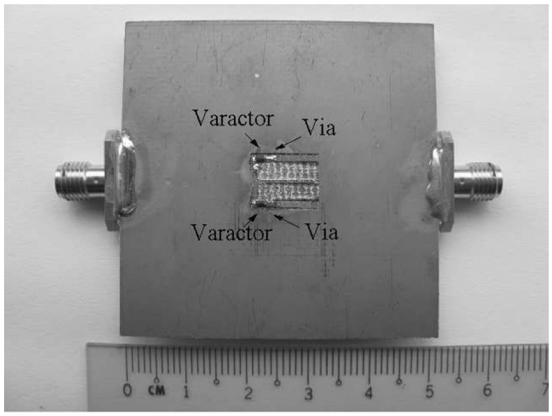

Fig. 17. Photograph of the ground plane side of the fabricated tunable E-shaped bandstop resonator with varactors and dc supply.

range of 12.4%. As can be seen in Fig. 14, the resonant frequency increases with an increase in the dc voltage (a decrease in total capacitance of the varactors) within the expected tuning range (1.80–2.66 GHz). The measured results when the dc bias is 0 and 15 V are in good agreement with the simulated results of the equivalent circuit in Fig. 13. This indicates the accuracy of the proposed equivalent circuit in Fig. 12(b) for the E-shaped structure with mounted lumped components across the gap. Based on the measured S-parameters, the Q factors of the implemented tunable resonator are calculated for different dc supply voltages. The Q factor varies from 18.65 to 31.67 when the dc supply is changed from 0 to 15 V. Comparing to the E-shaped structure in Fig. 3(b), the tunable resonator has a lower Q factor. This is probably due to the loss of the varactors and the dc supply circuits that are used for tuning.

In comparison to a T-shaped structure, their tuning ranges are comparable, while this proposed E-shaped structure is much smaller in physical size when the center frequency of tuning is set to be the same. Furthermore, only the E-shaped structure is able to accommodate lumped components even when the length of the arm, x, is very small.

V. Conclusion

In this paper, a new E-shaped patterned ground structure is proposed by modifying the most recently developed T-shaped resonator and adopting the U-slot resonator geometry. A detailed literature review on patterned ground structures is presented. This proposed bandstop resonator has an E-shaped patterned ground plane. It is designed, analyzed, and compared to the patterned ground structures in the literature. When all these structures are designed to resonate at the same frequency of 5 GHz, the proposed structure has the smallest circuit area among all the structures. It takes less than 50% of the area of all other resonant cells. Moreover, it has the sharpest transition knees and the highest Q factor. It is comparable to the best although the attenuation at the resonant frequency and the performance in the upper passband is not idea. Besides the comparison, the effect of the dimensions of the proposed structure on its performance is also studied in details. This proposed structure is applied to the design of a tunable bandstop resonator. It is fabricated and tested, achieving a compact physical size and a wide tuning range of 12.4%. An accurate circuit model is proposed to ease the study of the tuning behavior of the structure. Simulation and measurement results shows good agreement with each other, verifying the accuracy of the proposed circuit model and the superior performance of the proposed patterned ground structure.

Acknowledgment

The authors would like to thank Dr. B.-I. Wu, Center for Electromagnetic Theory and Applications, Department of Electrical Engineering and Computer Science, Massachusetts Institute of Technology (MIT), Cambridge, for his valuable discussions. The authors would also like to thank the anonymous reviewers for their valuable suggestions.

References

[1] V. Radisic, Y. Qian, R. Coccioli, and T. Itoh, "Novel 2-D photonic bandgap structure for microstrip lines," *IEEE Microw. Guided Wave Lett.*, vol. 8, no. 2, pp. 69–71, Feb. 1998.

[2] F. Falcone, T. Lopetegi, and M. Sorolla, "1-D and 2-D photonic bandgap microstrip structures," *Microw. Opt. Technol. Lett.*, vol. 22, no. 6, pp. 411–412, Sep. 1999.

[3] S. Y. Huang and Y. H. Lee, "Tapered dual-plane compact electromagnetic band-gap microstrip filter structure," *IEEE Trans. Microw. Theory Tech.*, vol. 53, no. 9, pp. 2656–2664, Sep. 2005.

[4] C. Caloz, H. Okabe, T. Iwai, and T. Itoh, "A simple and accurate model for microstrip structures with slotted ground plane," *IEEE Microw. Wireless Compon. Lett.*, vol. 14, no. 4, pp. 133–135, Apr. 2004.

[5] D. Ahn, J. Park, C. Kim, J. Kim, Y. Qian, and T. Itoh, "A design of the low-pass filter using the novel microstrip defected ground structure," *IEEE Trans. Microw. Theory Tech.*, vol. 49, no. 1, pp. 86–93, Jan. 2001.

[6] V. Radisic, Y. Qian, and T. Itoh, "Broad-band power amplifier using dielectric photonic bandgap structure," *IEEE Microw. Guided Wave Lett.*, vol. 8, no. 1, pp. 13–14, Jan. 1998.

[7] A. B. Abdel-Rahman, A. K. , A. Boutejdar, and A. S. Omar, "Control of bandstop response of hi–lo microstrip low-pass filter using slot in ground plane," *IEEE Trans. Microw. Theory Tech.*, vol. 52, no. 3, pp. 1008–1013, Mar. 2004.

[8] C. Kim, J. Lim, S. Nam, K. Kang, J. Park, G. Kim, and D. Ahn, "The equivalent circuit modeling of defected ground structure with spiral shape," in *IEEE MTT-S Int. Microw. Symp. Dig.*, Jun. 2002, vol. 3, pp. 2125–2128.

[9] M. K. Mandal and S. S. , "A novel defected ground structure for planar circuits," *IEEE Microw. Wireless Compon. Lett.*, vol. 16, no. 2, pp. 93–95, Feb. 2006.

[10] C. C. Wong and C. E. Free, "DGS pattern with enhanced effective capacitance," *Electron. Lett.*, vol. 42, no. 8, pp. 470–471, 2006.

[11] A. M. E. Safwat, F. Podevin, P. Ferrari, and A. Vilcot, "Tunable bandstop defected ground structure resonator using reconfigurable dumbbell-shaped coplanar waveguide," *IEEE Trans. Microw. Theory Tech.*, vol. 54, no. 9, pp. 3559–3564, Sep. 2006.

[12] X. Wang, B. Wang, H. Zhang, and K. J. Chen, "A tunable bandstop resonator based on a compact slotted ground structure," *IEEE Trans. Microw. Theory Tech.*, vol. 55, no. 9, pp. 1912–1917, Sep. 2007.

[13] D. Woo, T. Lee, J. Lee, C. Pyo, and W. Choi, "Novel U-slot and V-slot DGSs for bandstop filter with improved Q factor," *IEEE Trans. Microw. Theory Tech.*, vol. 54, no. 6, pp. 2840–2847, Jun. 2006.

[14] H. Liu, Z. Li, X. Sun, and J. Mao, "An improved 1-D periodic defected ground structure for microstrip line," *IEEE Microw. Wireless Compon. Lett.*, vol. 14, no. 4, pp. 180–182, Apr. 2004.

[15] H. Chen, T. Huang, C. Chang, L. Chen, N. Wang, Y. Wang, Y. Wang, and M. Houng, "A novel cross-shape DGS applied to design ultra-wide stopband low-pass filters," *IEEE Microw. Wireless Compon. Lett.*, vol. 16, no. 5, pp. 252–254, May 2006.

[16] A. B. Abdel-Rahman, A. K. Verma, A. Boutejdar, and A. S. Omar, "Control of bandstop response of hi-lo microstrip low-pass filter using slot in ground plane," *IEEE Trans. Microw. Theory Tech.*, vol. 52, no. 3, pp. 1008–1013, Mar. 2004.

[17] D. H. Staelin, A. W. Morgenthaler, and J. A. Kong, *Electromagnetic Waves.*. Upper Saddle River, NJ: Prentice-Hall, 1994, pp. 349–355.

[18] Q. Xue, K. M. Shum, and C. H. Chan, "Novel 1-D microstrip PBG cells," *IEEE Microw. Guided Wave Lett.*, vol. 10, no. 10, pp. 403–405, Oct. 2000.

[19] *1.25 Gamma Hyperabrupt Varactors SPICE Model*. Westford, MA: MDT Corporation, 2008.

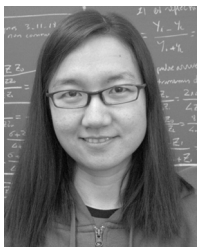

Shao Ying Huang (S'06–M'08) received the B.Eng. and M.Eng. degree from Nanyang Technological University, Singapore, in 2003 and 2005, respectively, and is currently working toward the Ph.D. degree at the School of Electrical and Electronic Engineering, Nanyang Technological University, Singapore.

She is currently a Visiting Student with the Center for Electromagnetic Theory and Applications, Department of Electrical Engineering and Computer Science, Massachusetts Institute of Technology (MIT), Cambridge. Her research interests include electromagnetic properties of periodic structures.

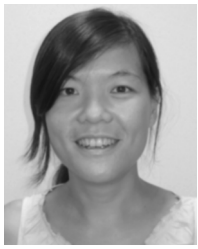

Yee Hui Lee (S'95–M'96) received the B.Eng. and M.Eng. degree from Nanyang Technological University, Singapore, in 1996 and 1998, respectively, and the Ph.D. degree from the University of York, York, U.K., in 2002.

In July 2002, she joined the School of Electrical and Electronic Engineering, Nanyang Technological University. Her research interests are wave propagation, evolutionary techniques, computational electromagnetics, and antenna designs.